

## Freezing Point Depressions of Aqueous MEA, MDEA, and MEA–MDEA Measured with a New Apparatus

Philip Loldrup Fosbøl,\* Mikkel Gielsager Pedersen, and Kaj Thomsen

Center for Energy Resources Engineering, Department of Chemical and Biochemical Engineering, Technical University of Denmark, Søtofts Plads Building 229, 2800 Kongens Lyngby, Denmark

**ABSTRACT:** Freezing points for aqueous monoethanolamine (MEA), methyl diethanolamine (MDEA), and MEA–MDEA solutions were measured in the concentration range from 0 to 0.4 mass fractions of the alkanolamines. For the aqueous MEA–MDEA system, freezing points for 1:4, 1:2, 1:1, 2:1, and 4:1 molar ratios of MEA/MDEA were determined. The experimental values indicate that the MDEA–water interaction is stronger than the MEA–water interaction. Measurements were carried out by a new modified Beckmann apparatus, which has not previously been described. The apparatus and method proved to have good repeatability and accuracy. A correlation of the freezing points as functions of the solution composition was made. Measurements of aqueous MEA and aqueous MDEA were compared to experiments found in the open literature.

### INTRODUCTION

Absorption with aqueous solutions of alkanolamines is an important operation for removal of acid gases. In recent years, the possibility of removing CO<sub>2</sub> from flue gas of fossil fuelled electric power plants by postcombustion capture has been given increased attention due to global warming. The solvent most commonly used for CO<sub>2</sub> absorption is a 0.30 mass fraction aqueous solution of MEA.

Primary alkanolamines, such as MEA, and secondary alkanolamines, such as diethanolamine (DEA), are very reactive toward CO<sub>2</sub>, resulting in high CO<sub>2</sub> removal rates on absorption. Primary and secondary alkanolamines form carbamates with CO<sub>2</sub>. The strong bonds in these molecules need to be broken in order to regenerate the amine solution. As a consequence the amines are costly in regard to energy consumption during desorption of CO<sub>2</sub>.

Tertiary alkanolamines such as MDEA do not form carbamates. This is due to the sterical hindrance in the reaction between amine and CO<sub>2</sub>. Unfortunately these amines have typically lower reaction rates for CO<sub>2</sub> removal than the primary and secondary amines. The benefit is less energy required on regeneration since the carbamate reaction does not need to be reversed.

Pilot plant studies of postcombustion capture have been carried out with aqueous solutions of the mixed MEA/MDEA solvent, e.g., Idem et al.<sup>1</sup> These studies show that there is a potential for reducing the energy required for regenerating the solvent with mixed MEA/MDEA. The goal has been to blend primary or secondary alkanolamines with tertiary alkanolamines, obtaining the most favorable properties of both amine types: high reaction rate from the primary/secondary amines and no carbamate formation for tertiary amines. The resulting solvent should retain the desired properties of high CO<sub>2</sub> loading capacity, fast reaction rate, together with better energy efficiency.

Several electrolyte thermodynamic models have been applied to the alkanolamine–H<sub>2</sub>O–CO<sub>2</sub> system. The electrolyte

NRTL model was applied by Hessen et al.,<sup>2</sup> and the Extended UNIQUAC model was applied by Faramarzi et al.<sup>3,4</sup> Both models are activity coefficient models for electrolytes which utilize interaction parameters fitted for each pair of species from binary or ternary data.

Only a few measurements are available for the MEA–MDEA–water ternary system. The solubility of CO<sub>2</sub> in aqueous alkanolamine mixtures was reported by Dawodu et al.<sup>5</sup> and Shen et al.<sup>6</sup> Freezing points of aqueous solutions of single alkanolamines were reported by Chang et al.<sup>7</sup> The alkanolamines measured by Chang et al.<sup>7</sup> were MEA, DEA, triethanolamine (TEA), MDEA, dimethylmonoethanolamine (DMMEA), and diglycolamine (DGA). Most measurements by Chang et al.<sup>7</sup> were obtained by using a modified Beckmann apparatus<sup>8</sup> though some measurements were made with an osmometer. The freezing point data for the H<sub>2</sub>O–MDEA system from Chang et al.<sup>7</sup> are not conclusive. Parts of the measurements are divided into two series forming a curve that separates into two branches, as can be seen in Figure 1. An error of this magnitude can have considerable effect, for the estimation of the loss of water, in the process of stripping the CO<sub>2</sub> from the amine solution. The uncertainty of the two branches can result in a difference in water activity up to 3.5%. This is determined by considering the reaction H<sub>2</sub>O(s) ↔ H<sub>2</sub>O(l) with the equilibrium constant of

$$K = a_{\text{H}_2\text{O}(l)} \quad (1)$$

using the relation for  $K$  from either of the two branches. Especially, the binary interaction between amine molecules and water during thermodynamic modeling will be noticeably affected by this difference. The equilibrium constant is calculated as function of temperature using the reaction standard state

**Special Issue:** John M. Prausnitz Festschrift

**Received:** October 5, 2010

**Accepted:** December 9, 2010

**Published:** January 24, 2011

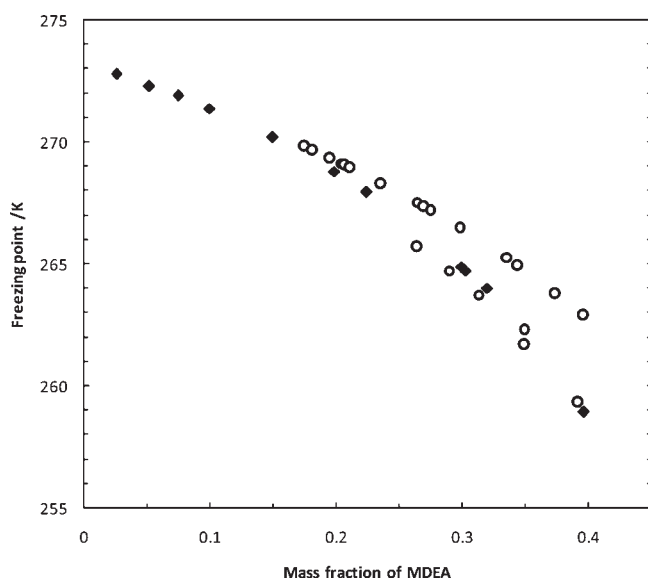


**Figure 1.** Freezing points of MDEA–water. O, Chang et al.<sup>7</sup>; ◆, present work.

Gibbs energy,  $\Delta_r G_{T_0, P_0}^\circ$ , and enthalpy,  $\Delta_r H_{T_0, P_0}^\circ$ , at reference temperature and pressure  $T_0 = 298.15$  K and  $P_0 = 1$  bar

$$\begin{aligned}
 R \ln K = & -\Delta_r G_{T_0, P_0}^\circ / T_0 + \Delta_r H_{T_0, P_0}^\circ \left( \frac{1}{T_0} - \frac{1}{T} \right) \\
 & + \Delta_r a \left( \ln \frac{T}{T_0} + \frac{T_0}{T} - 1 \right) + 0.5 \Delta_r b \left( \frac{(T - T_0)^2}{T} \right) \\
 & + \frac{\Delta_r c}{T_\Theta} \left( \frac{T - T_\Theta}{T} \ln \frac{T - T_\Theta}{T_0 - T_\Theta} + \ln \frac{T_0}{T} \right) \quad (2)
 \end{aligned}$$

where  $\Delta_r a$ ,  $\Delta_r b$ , and  $\Delta_r c$  are determined similar to the reaction Gibbs energy and enthalpy using heat capacity correlation coefficients from the correlation  $C_{p,i}^\circ = a_i + b_i T + c_i / (T - T_\Theta)$ ,  $T_\Theta = 200$  K. All the used constants and properties of  $\text{H}_2\text{O}$  (s) and  $\text{H}_2\text{O}$  (l) are given by Fosbøl et al.<sup>9</sup>

The above-mentioned difference shows that there is clearly a need of accurate freezing point data for the MDEA–water system. In addition, there is a need for MEA–MDEA–water freezing point data, from which the interactions of the two amines can be determined.

The aim of this work has been to develop a simple, but accurate apparatus for measurement of freezing point depression. The main focus was to determine a precise freezing point curve in the MDEA–water system. Additionally the aim has been to determine the interaction between MEA and MDEA in aqueous solutions. This was done by measuring freezing points in the binary MEA–water and the ternary MEA–MDEA–water system.

## EXPERIMENTAL DETAILS

**Materials.** MEA and MDEA together with the NaCl for calibration were purchased from Sigma-Aldrich at a purity of  $\geq 0.99$ . Deionized water was used for preparation of sample solutions using an analytical weight with an accuracy of  $\pm 0.1$  mg. The size of the binary MDEA/MEA batches before dilution was approximately 100 g. The final size of the various aqueous MDEA/MEA solutions was approximately 30 g.

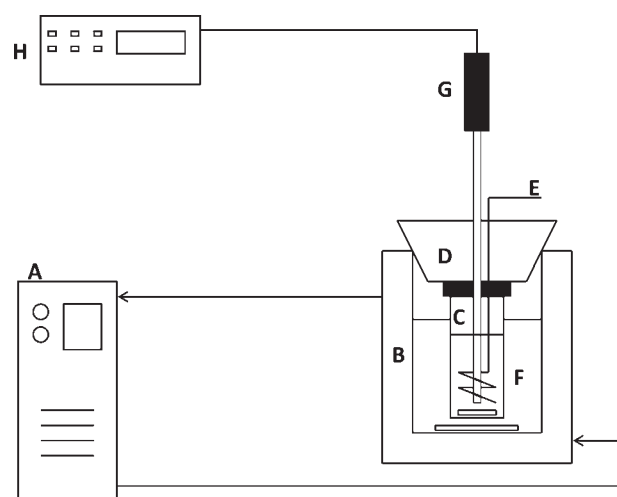


**Figure 2.** Experimental setup. A, Thermostatic bath with ethanol; B, cooling jacket; C, sample glass with magnetic stirrer; D, rubber stopper with sample glass lid; E, device for manual stirring; F, controlled temperature ethanol bath with magnetic stirrer; G, Pt100 thermometer; H, data acquisition unit.

**Apparatus.** The freezing points were measured using a modified Beckmann apparatus. The experimental setup is shown in Figure 2.

The temperature was controlled by a Lauda RE 110 thermostatic bath, which is able to lower the temperature of the refrigerant to approximately 233 K (A). Ethanol was used as refrigerant. The sample temperature was recorded by an Agilent 34970A data acquisition unit in connection to a PC (H) using a Pt100 DIN 1/10 custom-made Beta temperature sensor (G). It was made with a handle, 30 cm in length, and a 0.8 cm Pt100 element pushed inside a stainless steel container to the tip of the probe. The small element insures that the temperature is measured in the liquid sufficiently far away from the surface. Freezing point measurements were carried out in a sample glass (C) fitted with a magnetic stirrer, a device for manual stirring (E), as well as the temperature sensor (G). The lid of the container was mounted to a big rubber stopper (D). Both lid and the rubber stopper were penetrated by the temperature probe and magnetic stirrer. The total pressure was the atmospheric pressure under the experimental conditions. The sampling glass container was placed in a controlled temperature bath (F). The constant temperature was maintained by the cooling jacket (B). The cooling jacket is identical to those designed by Fosbøl et al.<sup>10</sup> used in analysis of salt solubility. An additional magnetic stirrer was placed in the cooling liquid in order to ensure homogeneous temperature conditions outside the sample glass. The Agilent data acquisition unit was calibrated against recommended freezing point values of aqueous NaCl of Clarke and Glew.<sup>11</sup> Seven sample solutions for the calibration were prepared in the concentration range from 0 to 0.2 mass fraction with freezing points between (0 and 253.15) K ( $-20$  °C). 10-fold measurements were made of the calibration samples. The standard deviation of the calibration measurements did not exceed 0.03 K.

**Experimental Method.** The measurement of a sample was carried out as follows. Samples of binary aqueous MEA and aqueous MDEA solutions were prepared in mass fractions of 0 to 0.40. Ternary aqueous MEA–MDEA solutions were made by first preparing binary solutions of MEA and MDEA with a fixed molar ratio. These solutions were prepared with the molar ratios

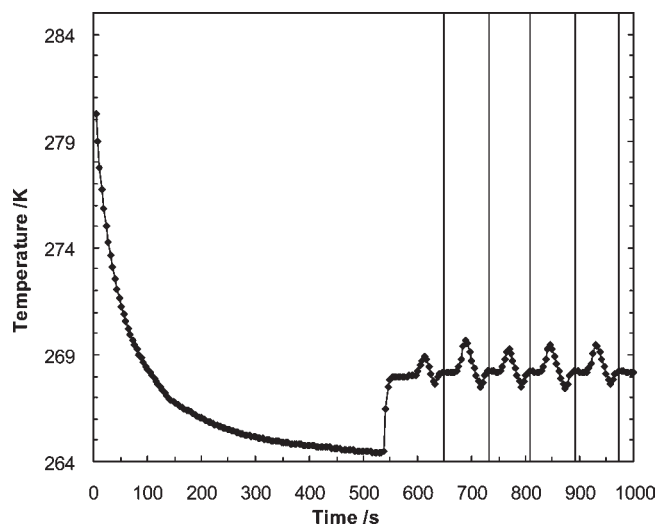


**Figure 3.** Measurement of freezing point. —◆—, Course of freezing point measurement. The points of which the freezing points were registered are marked by vertical lines.

1:4, 1:2, 1:1, 2:1, and 4:1 MEA/MDEA. Samples of aqueous MEA/MDEA solutions were then prepared of 0 to 0.40, mass fraction from the MEA/MDEA solutions by known dilution.

The temperature of the controlled temperature bath was adjusted to approximately 5 K below the expected freezing point of the sample. A total of (5 to 10) g of a solution was placed in a sample glass which was closed with a lid attached to the rubber stopper. The sample glass was then lowered into the controlled temperature bath. The development of the sample temperature was recorded every fourth second as shown by Figure 3.

During measurement, continuous magnetic as well as manual stirring were applied. Ice formation was registered at the rise of the sample temperature as the latent heat of fusion of liquid water was released. Figure 3 shows the course of measuring one freezing point repeated five times. From the start of the experiment at 0 s to approximately 540 s the sample is cooled. Hereafter the temperature rises abruptly to approximately 268 K due to ice formation.

A procedure is now followed as shown in Figure 4. The freezing point is recorded at 268.29 K at the time indicated by the vertical line in the figure. The next 15 s the temperature drops slightly from 268.29 K toward 268.2 K due to a change of the water concentration in the liquid phase from freezing out of ice.

The ice in the sample is melted by placing the glass in an ethanol bath at room temperature as indicated by the dotted part of the curve in Figure 4. This was obtained by “heating” a few seconds and visually inspecting the sample. Close to the point where all ice was melted, the heating could be done by holding the sample glass in the air while stirring and carefully watching the small remaining crystals. This way microscopic ice crystals were kept in solution as seed crystals by not heating the solution too much. It limits the subcooling during ice formation in the next measurement. By the above controlled presence of almost unnoticeable crystals between experiments in the sample, the repeatability of the measurements was ensured and a high degree of accuracy was obtained. For each sample, at least five measurements were made with an expected standard deviation less than 0.05 K.

Figure 3 shows the complete freezing point procedure. It should be noticed how at 100 s the freezing point is reached but

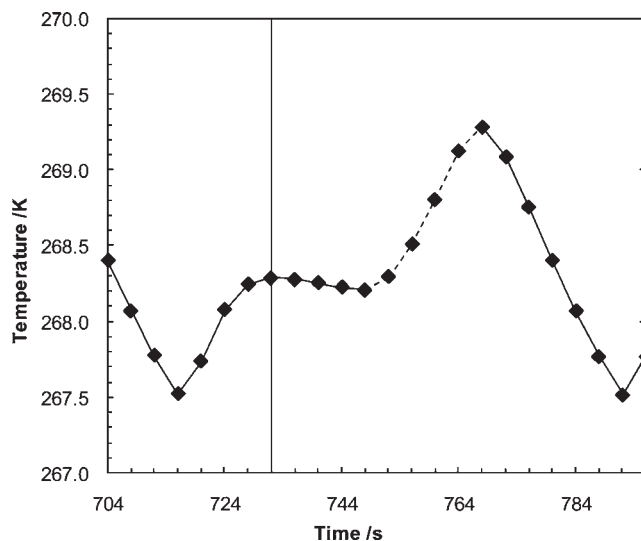


**Figure 4.** Measurement of freezing point. Enlargement from Figure 3 from (704 to 796) s. —◆—, Course of freezing point measurement. The point of which the freezing point was registered is marked by vertical lines. The dotted section of the temperature curve indicates the periods of the measurement for which the sample was heated externally.

**Table 1.** Experimental Measurements of the Freezing Point of the MEA–Water System from This Work

MEA concentration	freezing point	standard deviation
mass fraction	K	K
0.02489	272.45	0.01
0.05035	271.46	0.01
0.07539	270.70	0.003
0.09192	269.92	0.02
0.14119	267.81	0.008
0.14985	267.54	0.02
0.19845	264.79	0.01
0.21863	263.89	0.008
0.24666	261.62	0.05
0.29921	258.11	0.01
0.30649	256.88	0.05

ice is not formed. The solution is being subcooled. Suddenly at 540 s ice forms stochastically. The large subcooling results in inaccurate measurement of the freezing point, due to excess formation of ice. The noticeable amount of ice formed changes the liquid phase concentration and the first registered freezing point is therefore not accurate.

The first freezing point measurement, and experiments for which a high degree of subcooling was observed, were not included in the results. This is indicated in Figure 3 by the missing vertical line at the first freezing point.

## RESULTS AND DISCUSSION

Results of the experimental work are presented in the Tables 1, 2, and 3, and they are graphically displayed in Figures 1, 5, and 6. In Tables 1, 2, and 3 the composition of the freezing points of the samples are listed together with the standard deviations of 5-fold measurements. With the exception of three cases, all of the fifty-five

**Table 2. Experimental Measurements of the Freezing Point of the MDEA–Water System from This Work**

MDEA concentration	freezing point	standard deviation
mass fraction	K	K
0.02581	272.79	0.004
0.05173	272.31	0.03
0.07484	271.90	0.006
0.09979	271.39	0.02
0.14922	270.20	0.004
0.14999	270.19	0.007
0.19867	268.81	0.007
0.22464	267.95	0.01
0.30001	264.90	0.02
0.30272	264.73	0.01
0.31966	264.02	0.01
0.39655	258.95	0.07

**Table 3. Experimental Measurements of the Freezing Point of the MEA–MDEA–Water System from This Work<sup>a</sup>**

solution	MEA concentration	MDEA concentration	freezing point	standard deviation
	mass fraction	mass fraction	K	K
molar ratio 1:1	0.01699	0.03313	272.00	0.009
MEA/MDEA	0.03366	0.06563	270.72	0.01
	0.04955	0.09662	269.34	0.009
	0.06675	0.13016	267.52	0.02
	0.10327	0.20137	262.18	0.02
	0.11755	0.22920	259.17	0.02
molar ratio 1:2	0.00942	0.04619	271.97	0.008
MEA/MDEA	0.01830	0.08970	270.74	0.006
	0.02518	0.12340	269.62	0.009
	0.03398	0.16656	267.87	0.01
	0.05082	0.24911	263.22	0.05
	0.06089	0.29845	259.36	0.06
molar ratio 2:1	0.02800	0.02394	271.82	0.009
MEA/MDEA	0.05158	0.04411	270.59	0.02
	0.09126	0.07804	268.08	0.008
	0.11285	0.09651	266.36	0.01
	0.15875	0.13576	261.64	0.04
	0.21299	0.18215	253.21	0.08
molar ratio 1:4	0.00565	0.04410	272.19	0.02
MEA/MDEA	0.01133	0.08844	271.18	0.02
	0.01732	0.13517	269.79	0.01
	0.02307	0.18007	268.23	0.02
	0.03438	0.26831	263.81	0.04
	0.04469	0.34882	257.88	0.03
molar ratio 4:1	0.03257	0.01590	271.66	0.009
MEA/MDEA	0.06601	0.03221	270.28	0.03
	0.10740	0.05241	267.92	0.01
	0.13204	0.06444	266.32	0.008
	0.16902	0.08248	263.43	0.02
	0.19411	0.09473	261.03	0.01
	0.23267	0.11355	256.53	0.03
	0.25536	0.12462	253.00	0.06

<sup>a</sup>The mass fractions of the amines are listed. The remaining mass fraction is made up of water.

measurements performed in this work have standard deviations equal to or less than 0.05 K. The standard deviation has a tendency to increase with higher amine concentration. This can be a result of

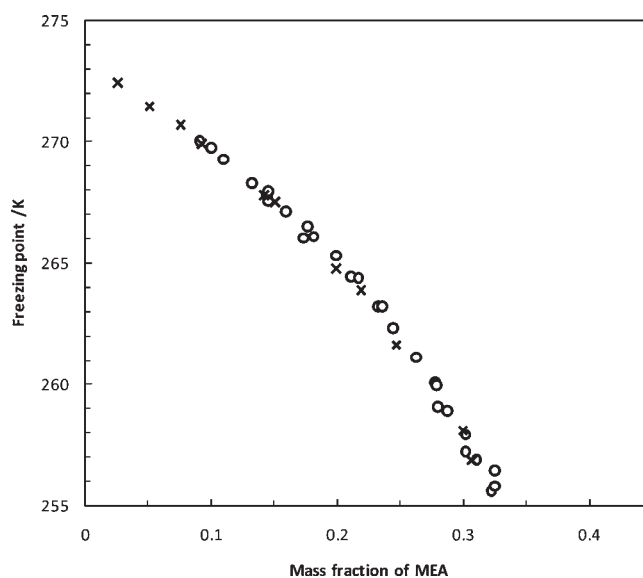


Figure 5. Freezing points. MEA–water. O, Chang et al.<sup>7</sup>; x, present work.

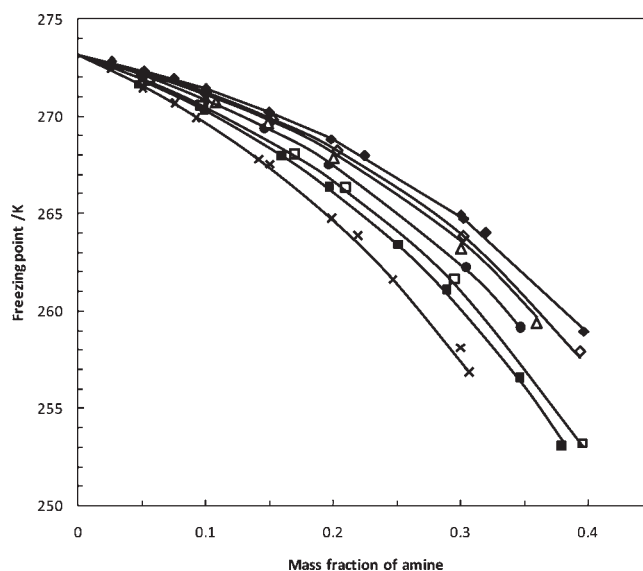
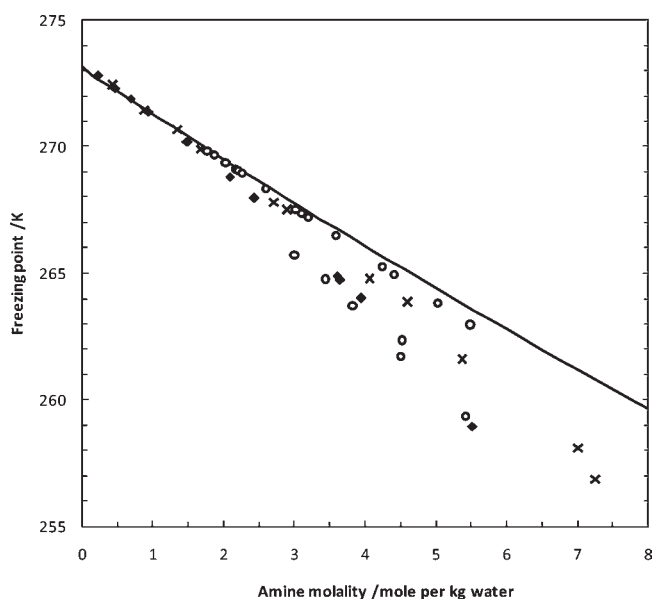


Figure 6. Freezing points of MEA–MDEA–water solutions measured in this work. ♦, MDEA; ◇, 1:4 molar ratio MEA/MDEA; △, 1:2 molar ratio MEA/MDEA; ●, 1:1 molar ratio MEA/MDEA; □, 2:1 molar ratio MEA/MDEA; ■, 4:1 molar ratio MEA/MDEA; ×, MEA. Equations 3 to 5 were used for calculating the lines.

the increased viscosity in the concentrated solution, which makes the mixing of the sample less efficient.

The MDEA–water freezing points in Figure 1 indicate that it is the lower of the two series of the data from Chang et al.<sup>7</sup> that is most accurate. The measurements of the MEA–water shown in Figure 5 are in good agreement with data of Chang et al.<sup>7</sup> in the full concentration range from 0 to 0.33 mass fractions. Figure 6 shows the measured binary and ternary freezing points found in this work. The binary solutions of aqueous MEA on a mass fraction basis have the lowest freezing points and the binary aqueous MDEA have the highest. The freezing points of the intermediate ternary amine mixtures are higher than those of aqueous MEA and lower than those of aqueous MDEA. It should be noticed, by comparing Figures 6 and 7, that the freezing points



**Figure 7.** Freezing points.  $\times$ , MEA–water, this work;  $\blacklozenge$ , MDEA–water, this work;  $\circ$ , MDEA–water, Chang et al.<sup>7</sup> The line indicates the freezing point of an ideal solution.

of aqueous MDEA is lower than aqueous MEA on a molal basis ( $\text{mol} \cdot (\text{kg H}_2\text{O})^{-1}$ ) but opposite on a mass fraction basis.

The freezing point of an ideal solution is shown by the line in Figure 7. It is calculated using eq 1 and mole fraction for the activity of water. The temperature dependence of the equilibrium constant is evaluated using the Gibbs–Helmholtz equation based on thermodynamic properties, heat capacity, and the equilibrium constant correlations presented by Fosbøl et al.<sup>9</sup> A noticeable deviation from ideality is observed above 1.5 *m* for both MEA–water and MDEA–water, greater deviation for the MDEA system compared to the MEA system. This indicates that the MDEA–water interaction is higher than the MEA–water interaction. The MDEA–water data from Chang et al.<sup>7</sup> is seen in Figure 7 as two series. The upper series is very similar to the ideal solution curve.

**Freezing-Point Correlation of H<sub>2</sub>O–MEA–MDEA.** A correlation for estimation of the freezing point depression from the sample composition was formulated as part of this work. It is represented by the following three equations.

$$\Delta T_{\text{MEA}} = c_1 \tilde{x}_{\text{MEA}} + c_2 \tilde{x}_{\text{MEA}}^2 \quad (3)$$

$$\Delta T_{\text{MDEA}} = c_3 \tilde{x}_{\text{MDEA}} + c_4 \tilde{x}_{\text{MDEA}}^2 \quad (4)$$

$$\Delta T_{\text{mix}} = \Delta T_{\text{MEA}} + \Delta T_{\text{MDEA}} + \tilde{x}_{\text{MEA}} \tilde{x}_{\text{MDEA}} (c_5 + c_6 \tilde{x}_{\text{MEA}}^2 + c_7 \tilde{x}_{\text{MDEA}}^2) \quad (5)$$

Equations 3 and 4 are the correlations of the freezing point depressions for the two binary systems MEA–water and MDEA–water, respectively. They each contain two parameters or a total of four parameters  $c_1$  to  $c_4$  in order to correlate the two binary systems. A correlation for estimating the freezing point depression of the ternary MEA–MDEA–water solution as a function of the composition is suggested in eq 5. The first two terms are the contribution from the freezing point of MEA and MDEA with a linear mixing rule based on eqs 3 and 4. The last term describes the interaction due to deviation from the linear mixing rule. This term contains three parameters,  $c_5$  to  $c_7$ . The

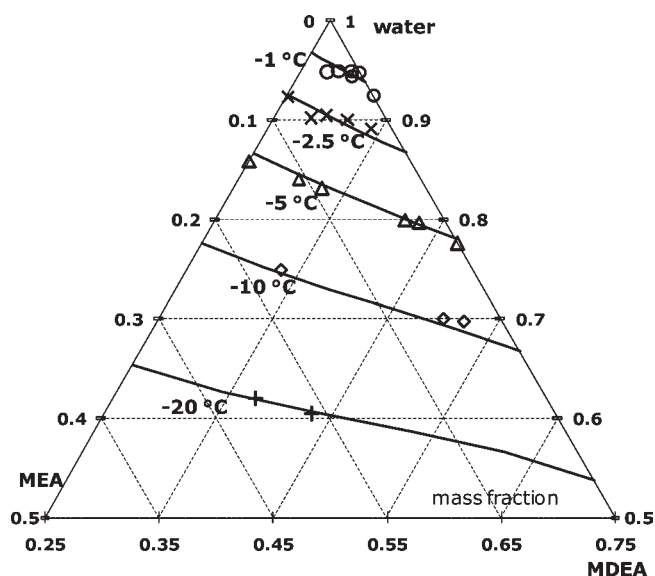


**Figure 8.** Isothermal freezing points of ice in MEA–MDEA–water solutions.  $\circ$ ,  $\times$ ,  $\Delta$ ,  $\diamond$ , and  $+$ , selected measurement of this work for the shown temperatures  $\pm 0.3$  K. Equations 3 to 5 were used for calculating the lines at the constant temperatures.

**Table 4.** Parameters for Freezing Point Correlation of eqs 3 to 5

model parameter	parameter value
	K
$c_1$	−99.012
$c_2$	−363.17
$c_3$	−94.601
$c_4$	−682.09
$c_5$	−566.42
$c_6$	1941.5
$c_7$	−3204.4

concentrations ( $\tilde{x}_i$ ) of MEA and MDEA in eqs 3 to 5 for the MEA–MDEA–water solutions are calculated according to

$$\tilde{x}_{\text{MEA}} = \frac{n_{\text{MEA}}}{n_{\text{MEA}} + n_{\text{water}}} \quad (6)$$

$$\tilde{x}_{\text{MDEA}} = \frac{n_{\text{MDEA}}}{n_{\text{MDEA}} + n_{\text{water}}} \quad (7)$$

where  $n_i$  is the moles of component  $i$  in the solution. The fitted parameters  $c_1$  to  $c_7$  are presented in Table 4 obtained by least-squares fitting between experimental and calculated freezing points.

Isothermal freezing point curves are shown in Figure 8 represented by the lines calculated using model eqs 3 to 5. The shown experimental data points are a maximum of  $\pm 0.3$  K from the calculated lines. The expected scatter is due to this difference in calculation and experimental conditions. The triangular diagram visualizes the solubility of ice in the ternary mixture of aqueous MEA–MDEA for water mass fractions  $> 0.5$ . A distinct linear behavior is noticed for the water saturated boundary lines running from the binary cases on the MEA–H<sub>2</sub>O axis to the MDEA–H<sub>2</sub>O axis. There is an acceptable accordance between the model and the experimental points.

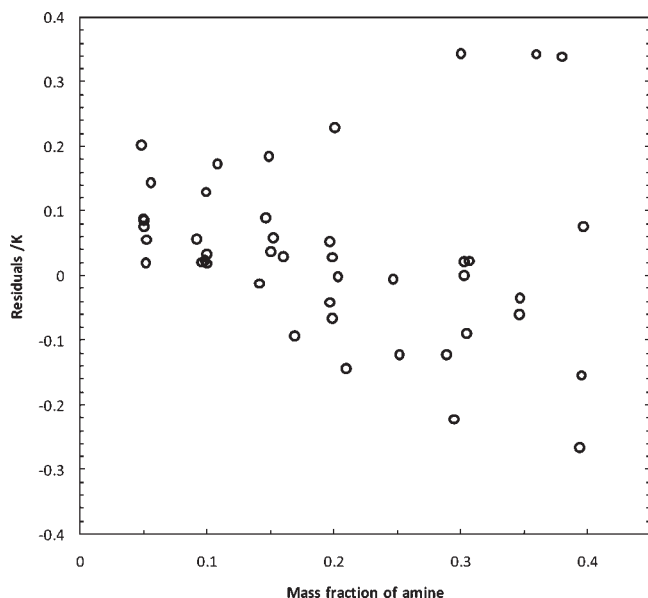


Figure 9. ○, Absolute deviations of values estimated by eq 5.

The model is valid from 0 to 0.12 mol fraction (0 to 0.3 mass fractions) of MEA and 0 to 0.09 mol fraction (0 to 0.4 mass fractions) of MDEA. It is expected to be valid also slightly outside this interval toward the eutectic point. Figure 9 shows that the residuals of the measured and estimated values are spread evenly around 0, and the accuracy is best at low concentrations. The mean absolute error for the correlation is 0.10 K.

## CONCLUSIONS

A new method and apparatus for accurate freezing points measurements were described. Freezing points of aqueous solutions of MEA, MDEA, and MEA–MDEA were measured in the concentration range from 0 to 0.4 mass fraction of the alkanolamines. In the aqueous mixtures of MEA and MDEA molar ratios between the amines were fixed. The molar ratios were 1:4, 1:2, 1:1, 2:1, and 4:1 MEA:MDEA. The experimental values indicate that the MDEA–water interaction is stronger than the MEA–water interaction. Based on the measurements, a correlation between freezing point and solution composition was formulated. The comparison between model and experimental work shows a linear trend in the isothermal phase boundary lines saturated in ice.

The measured data can be used when modeling the CO<sub>2</sub> absorption/desorption systems with mixed aqueous MEA/MDEA solvents. This can enhance the prediction of water loss, energy efficiency, and the energy requirements of the operation.

## AUTHOR INFORMATION

### Corresponding Author

\*E-mail: plf@kt.dtu.dk.

## ACKNOWLEDGMENT

As part of her studies, Randy Neerup measured some of the binary freezing point depression data presented in this work.

## REFERENCES

(1) Idem, R.; Wilson, M.; Tontiwachwuthikul, P.; Chakma, A.; Veawab, A.; Aroonwilas, A.; Gelowitz, D. Pilot Plant Studies of the

CO<sub>2</sub> Capture Performance of Aqueous MEA and Mixed MEA/MDEA Solvents at the University of Regina CO<sub>2</sub> Capture Technology Development Plant and the Boundary Dam CO<sub>2</sub> Capture Demonstration Plant. *Ind. Eng. Chem. Res.* **2006**, *45*, 2414–2420.

(2) Hessen, E. T. E.; Haug-Warberg, T.; Svendsen, H. F. H. The refined e-NRTL model applied to CO<sub>2</sub>–H<sub>2</sub>O–alkanolamine systems. *Chem. Eng. Sci.* **2010**, *65*, 3638–3648.

(3) Faramarzi, L.; Kontogeorgis, G. M.; Thomsen, K.; Stenby, E. H. Extended UNIQUAC model for thermodynamic modeling of CO<sub>2</sub> absorption in aqueous alkanolamine solutions. *Fluid Phase Equilib.* **2009**, *282*, 121–132.

(4) Faramarzi, L.; Kontogeorgis, G. M.; Thomsen, K.; Stenby, E. H. Thermodynamic modeling of the solubility of CO<sub>2</sub> in aqueous alkanolamine solutions using the extended UNIQUAC model application to monoethanolamine and methyldiethanolamine. *Energy Procedia* **2009**, *1*, 861–867.

(5) Dawodu, O. F.; Meisen, A. Solubility of carbon dioxide in aqueous mixtures of alkanolamines. *J. Chem. Eng. Data* **1994**, *39*, 548–552.

(6) Shen, K.; Li, M. Solubility of carbon dioxide in aqueous mixtures of monoethanolamine with methyldiethanolamine. *J. Chem. Eng. Data* **1992**, *37*, 96–100.

(7) Chang, H.; Posey, M.; Rochelle, G. T. Thermodynamics of alkanolamine–water solutions from freezing point measurements. *Ind. Eng. Chem. Res.* **1993**, *32*, 2324–2335.

(8) Beckmann, E. Determination of molecular weights VII. *Z. Phys. Chem.* **1903**, *44*, 161–196.

(9) Fosbøl, P. L.; Thomsen, K.; Stenby, E. H. Modeling of the Mixed Solvent Electrolyte System CO<sub>2</sub>–Na<sub>2</sub>CO<sub>3</sub>–NaHCO<sub>3</sub>–Monoethylene Glycol–Water. *Ind. Eng. Chem. Res.* **2009**, *48*, 4565–4578.

(10) Fosbøl, P. L.; Thomsen, K.; Stenby, E. H. Solubility Measurements in the Mixed Solvent Electrolyte System Na<sub>2</sub>CO<sub>3</sub>–NaHCO<sub>3</sub>–Monoethylene Glycol–Water. *Ind. Eng. Chem. Res.* **2009**, *48*, 2218–2228.

(11) Clarke, E. C. W.; Glew, D. N. Evaluation of the thermodynamic functions for aqueous sodium chloride from equilibrium and calorimetric measurements below 154 °C. *J. Phys. Chem. Ref. Data* **1985**, *14*, 489–610.